iJRASET
International Journal For Research in Applied Science and Engineering Technology

INTERNATIONAL JOURNAL FOR RESEARCH

IN APPLIED SCIENCE & ENGINEERING TECHNOLOGY

Volume: 6 **Issue:** I **Month of publication:** January 2018

DOI: http://doi.org/10.22214/ijraset.2018.1441

www.ijraset.com

Call: 08813907089 | E-mail ID: ijraset@gmail.com

International Journal for Research in Applied Science & Engineering Technology (IJRASET)
ISSN: 2321-9653; IC Value: 45.98; SJ Impact Factor :6.887
Volume 6 Issue I, January 2018- Available at www.ijraset.com

Preparation and Characterisation of Nickel Doped Zinc Oxide Thin Films in comparison to ZnO Thin Films by Sol-Gel Method

Anup Kumar Das
Department of Physics, P. K. College, Contai, India.

Abstract: ***The aim to study the optical and structural properties of sol gel derived $Zn_{1-x}Ni_xO(x=0.01)$ thin films by spin coating technique with systematic investigation have been carried out. Zinc acetate dihydrate and nickel acetate tetra hydrate are used as the precursor material and dopant, respectively. The thin films of nickel doped ZnO are deposited onto glass substrate in room temperature and as-grown film is sintered at 100 ^oC for 5 minutes and then post annealed in air at 600 ^oC for 1 hour. The optical properties like absorbance, transmittance and hence band gap energy are measured by double beam spectrophotometer which show transmittance decreases and gap energy increases with respect to ZnO thin film. The both thin films exhibit high transparency above 70% for Ni doped ZnO and above 80% for undoped ZnO in visible region of optical spectrum. X-ray diffraction (XRD) studies on the films show the polycrystalline nature with hexagonal wurtzite structure. The crystallite sizes of the films are estimated using the Debye-Scherrer's formula and have shown 43.29 nm for 002 plane. The lattice parameters a, c of Ni doped ZnO slightly increases and crystallite size decreases with respect to undoped ZnO. The calculated value of a, c and c/a of 1% Ni doped ZnO are respectively, 3.266 Å, 5.224 Å and 1.599. The optical band gap energies of the films are observed to vary from 3.21 eV to 3.23 eV for ZnO and Ni doped ZnO and found to be direct allowed transition. The micrographs by high resolution transmission electron microscopy (HR-TEM) show grains with hexagonal structure of broad particle size distribution.***
Keywords: Sol-gel, Spin coating, Thin films, ZnNiO, XRD, HR-TEM, Optical band gap.

I. INTRDUCTION

Among II-IV semiconductors, Nickel doped zinc oxide is a versatile multifunctional compound with direct wide band gap (3.37eV at 300k) and large excitonic binding energy (60 meV). This semiconductor has several favourable properties, including good transparency, high electron mobility, strong room temperature luminescence, outstanding electro-optic and piezoelectric properties, and excellent chemical stability which can be useful in emerging applications of electronics and optoelectronics [1]- [5]. Ni doped ZnO thin films have been widely used for many devices application such as light emitting diodes [6], nanolasers [7] and have been recognized as spintronic material [8]. Also various biological, chemical and gas sensors [9] are based on ZnO thin film. Thin films of ZnNiO can be prepared by various techniques; among them are sputtering [10]-[11], metal-organic chemical vapour deposition (MOCVD) [12], pulse laser deposition (PLD) [13], spray pyrolysis [14] and sol-gel method [15]-[19] have studied structural and optical properties of nano crystalline ZnNiO thin films derived from clear emulation of nano-crystallite Ni doped ZnO nano crystals. Compare to the other processes, the sol-gel process has the advantages of control ability of chemical compositions due to its simplicity in processing and cost effective. Properties of ZnNiO thin films show dependence on the technique used apart from doping to increase the functionality of Ni doped ZnO thin film, the effect of preparation conditions on the properties have to be considered for its effective technological applications. In the present work sol-gel spin coating process is employed for film preparation. Zinc acetate dihydrate and nickel acetate tetra hydrate were used as the precursor material and dopant, respectively. The effects of annealing on the structural and optical properties of Ni doped ZnO thin films in comparison to ZnO thin films at 600 ^oC were studied. Double beam spectrophotometer was used for optical properties as well as XRD and HR-TEM were used for structural properties of Ni doped ZnO.

II. EXPERIMENTAL

Nickel doped ZnO thin films were prepared on glass substrate ($5X2.5cm^2$) by sol-gel spin coating technique by using ethanol [C_2H_5OH] as solvent. The glass substrates were cleaned with soap solution followed by ultrasonication in water for 1 hour. Then the substrates were cleaned successively in distilled water and in acetone. For this purpose 0.5 mole high purity zinc acetate dihydrate (ZAD) [$Zn(CH_3COO)_2.\ 2H_2O$] and appropriate proportion for 1% mole fraction of nickel acetate tetrahydrate (NAT)

[$Ni(CH_3COO)_2$. $4H_2O$] were used to prepare Ni doped ZnO thin films. Mono-ethanolamine (MEA) [C_2H_7NO] was used as stabilizing agent. Appropriate quantity of ZAD and NAT were mixed in 25 ml of ethanol and was stirred by magnetic stirrer at 60 ^oC until no solid particulates were found. Then the MEA was dropped to the bluish solution until a clear sol was appeared and the as-prepared solution was stirred at same temperature for 1 hour until a homogeneous sol was obtained. Then the freshly prepared sol was dropped onto a pre dried clean glass substrate using spin coating technique in room temperature with a rate of 3000 rpm in 30 sec. The as-coated film was sintered at 100 ^oC for 5 minutes immediately to evaporate the solvent. The process was repeated to obtain the workable thickness of the film up to seven coating layers. Then, the film is annealed in air at 600 ^oC for 1 hour in a tube furnace to reach the crystal phase. The flow chart is shown in Fig.

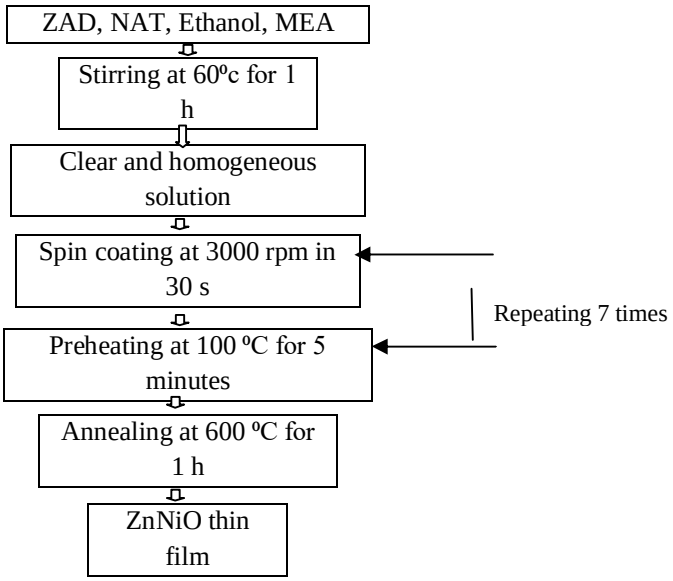

Fig1: The flow chart of methodology for preparation of ZnNiO thin film.

The optical measurements were carried out at room temperature using UV-VIS double beam spectrophotometer (Systronics 2202) in the wavelength range of 210nm – 550nm. The XRD [X'Pert High score plus, PANalytical] pattern was obtained with CuK_α radiation (λ=1.5406 Å) and the HR-TEM [JEM-2100F, Japan] images of Ni doped ZnO nanoparticles cluster were obtained from ultrasonicated sample on carbon grid that was prepared from as-grown thin film.

III. RESULTS AND DISCUSSION

A. Structural

Structural characterizations of Ni doped ZnO and undoped ZnO nanoparticles have been carried out by XRD and HR-TEM. The XRD spectrum for scanned angle (2θ) varying from 10^o to 90^o of ZnO and 1% Ni doped ZnO thin films grown at 600^oC is shown in Fig. 2. From this figure as-grown sample gives strong diffraction peaks at $2\theta = 31.65^o$, 34.314^o and 36.06^o for ZnO and 31.60^o, 34.306^o, 36.09^o for Ni doped ZnO which corresponds to (100), (002) and (101) peaks and showing growth of both crystallites of hexagonal wurtzite structure with higher degree of preference along the c-axis perpendicular to the substrate. The presence of prominent peaks shows that the film is polycrystalline in nature. The lattice constants a and c of the both nanocrystalline films were determined by using the Debye-Scherrer's formula.

$$a = \sqrt{\frac{1}{3}}\frac{\lambda}{\sin\theta} \quad (1)$$

$$c = \frac{\lambda}{\sin\theta} \quad (2)$$

Where, λ is the wavelength of X-ray and θ is the Bragg angle.

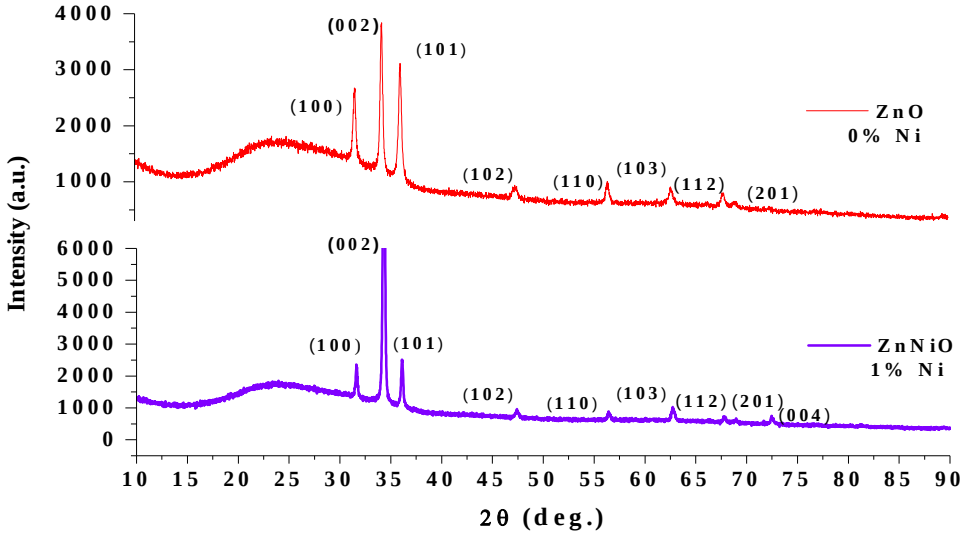

Fig2: XRD patterns of ZnO and ZnNiO thin films annealed at 600ºC.

The grain size (D) of ZnO nano crystals annealed at 600 °C was calculated using the following relation,

$$D = \frac{K\lambda}{\beta \cos \theta} \quad (3)$$

Where, K is constant and taken to be 0.94 [20] and β is the full width at half maximum (FWHM).

The dislocation density (δ) defined as the length of dislocation lines per unit volume is estimated using the relation

$$\delta = \frac{1}{D^2} \quad (4)$$

and the strain (€) of the thin films is estimated using the relation

$$€ = \frac{\beta Cos\ \theta}{4} \quad (5)$$

The lattice parameters (a and c) for hexagonal structure can also be calculated by using the relation (6).

$$\left(\frac{1}{d_{hkl}}\right)^2 = \frac{4}{3}\left(\frac{h^2+k^2+hk}{a^2}\right) + \frac{l^2}{c^2} \quad (6)$$

Where d_{hkl} be the lattice spacing with Miller indices hkl.

Table 1 shows the structural parameters and Table 2 shows the calculated lattice parameters of ZnO and 1% Ni doped ZnO as obtained from XRD. From Table 2 it shows that the lattice parameters (a, c) and hence unit cell volume (V) increases and crystallite size decreases for Ni doped ZnO with respect to undoped ZnO. From XRD parameters it was confirmed that Ni dopant does not alter so much ZnO structure, which due to the incorporation of Ni ions on Zn sites.

TABLE I

Structural parameters of ZnO and Ni doped ZnO thin films:

Thin films	% of Ni	Planes	Inter-Planer Spacing d (Å)	FWHM β ($\times 10^{-3}$) (rad.)	Dislocation Density δ ($\times 10^{14}$) (lines/m^2)	Strain € ($\times 10^{-4}$)
ZnO	0	(100)	2.827	1.458	0.938	3.50
		(002)	2.613	3.209	4.486	7.67
		(101)	2.491	2.918	3.672	6.94
$Zn_{0.99}Ni_{0.01}O$	1	(100)	2.831	0.1171	1.842	4.914
		(002)	2.614	0.2007	5.337	8.364
		(101)	2.489	0.1673	3.672	6.938

TABLE II
Calculated Lattice parameters of the ZnO and $Zn_{0.99}Ni_{0.01}O$ thin film:

Thin films	% of Ni	a (Å)	c (Å)	Unit Cell Volume V ($Å^3$)	Crystallite Size D (nm)
ZnO	0	3.262	5.222	144.36	47.22
$Zn_{0.99}Ni_{0.01}O$	1	3.266	5.224	144.75	43.29

1) *HR-TEM analysis:* Figures 3(a) and 3(b) show the low magnification TEM micrograph of cluster of Ni doped ZnO and undoped ZnO nanoparticles annealed at 600 ^oC. These micrographs show grains with hexagonal structure of broad particle size distribution.

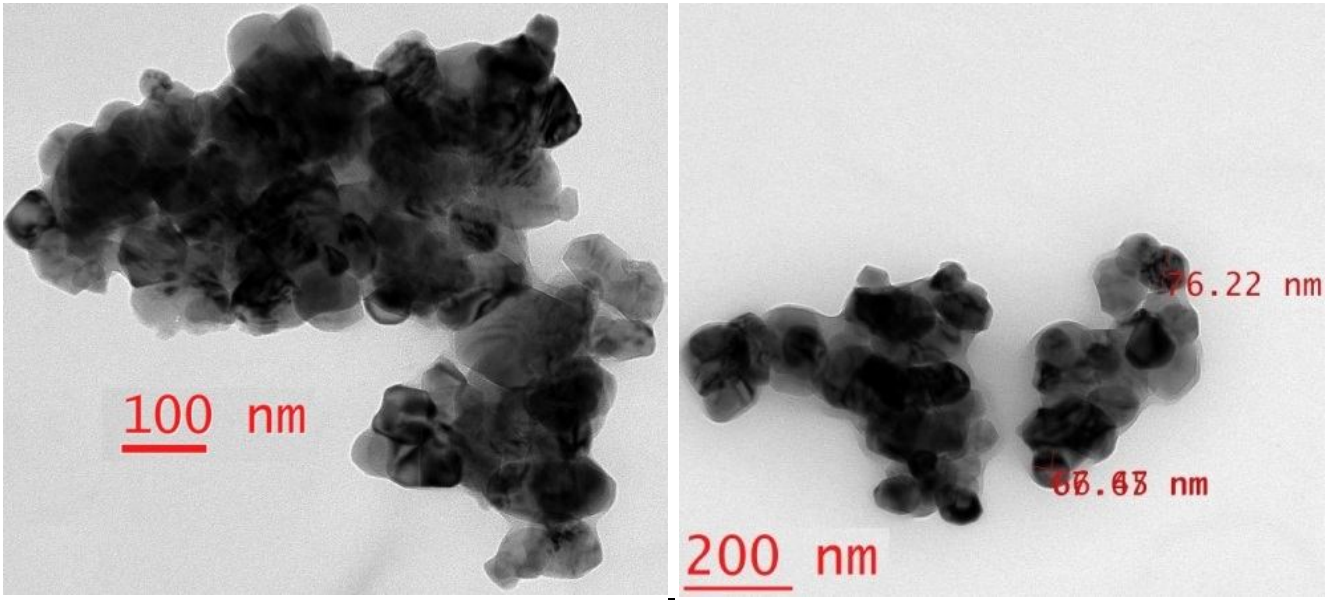

(a) (b)

Fig. 3: The cluster of low magnification TEM images of (a) ZnNiO and (b) ZnO nanoparticles

Crystallinity of each nanoparticles of Ni doped ZnO sample is confirmed from selected area electron diffraction (SAED) pattern as shown in Fig. 4. In this pattern bright spots make concentric rings that reveal the ZnNiO nanoparticles are polycrystalline nature.

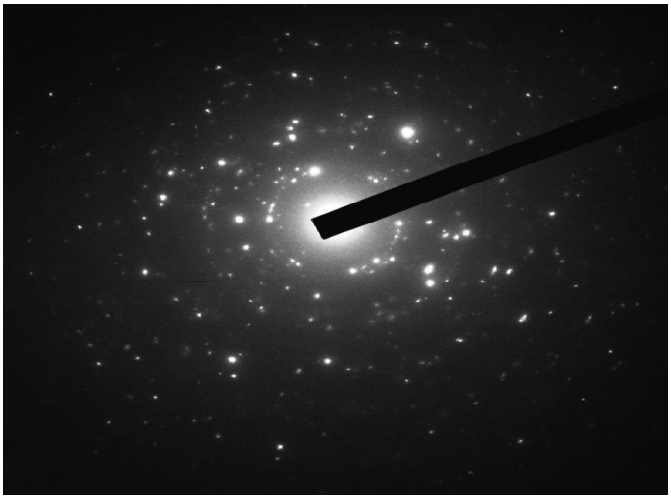

Fig. 4: SAED Pattern showing the polycrystalline Ni doped ZnO nanoparticles.

High resolution TEM image of the lattice planes of Ni doped ZnO sample is shown in Fig. 5(a). The corresponding equal spacing peaks arising from those parallel planes with inter planer spacing d= 2.338 Å is shown in Fig. 5(b).

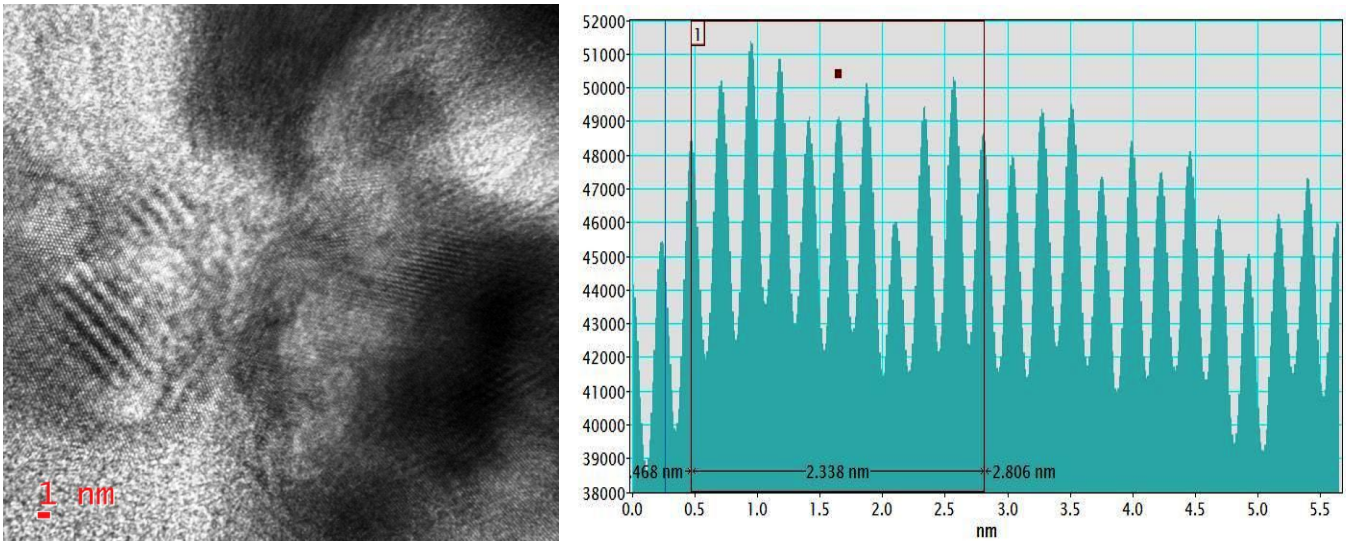

(a) (b)

Fig. 5: An atomic level lattice image of a magnified ZnNiO nanoparticles and histogram of d-spacing: (a) 1 nm regime and (b) corresponding peaks showing plane of inter planer spacing d= 2.338 Å.

B. Optical Properties

Figure 6 shows the optical transmittance spectrum of clear ZnO sol before spin coating process, nanocrystalline Ni doped ZnO and undoped ZnO thin films after annealing at 600 ^{o}C. It is clearly shown from these graphs that the clear sol of ZnO, undoped ZnO and doped ZnO thin films exhibit a high transmittance above 90%, 80% and 70%, respectively in visible region of optical spectrum. The position of the absorption edge is observed to be shifting towards lower wavelength side with increase in Ni concentration in ZnO indicating an increase in the band gap (Figure7) with Ni doping.

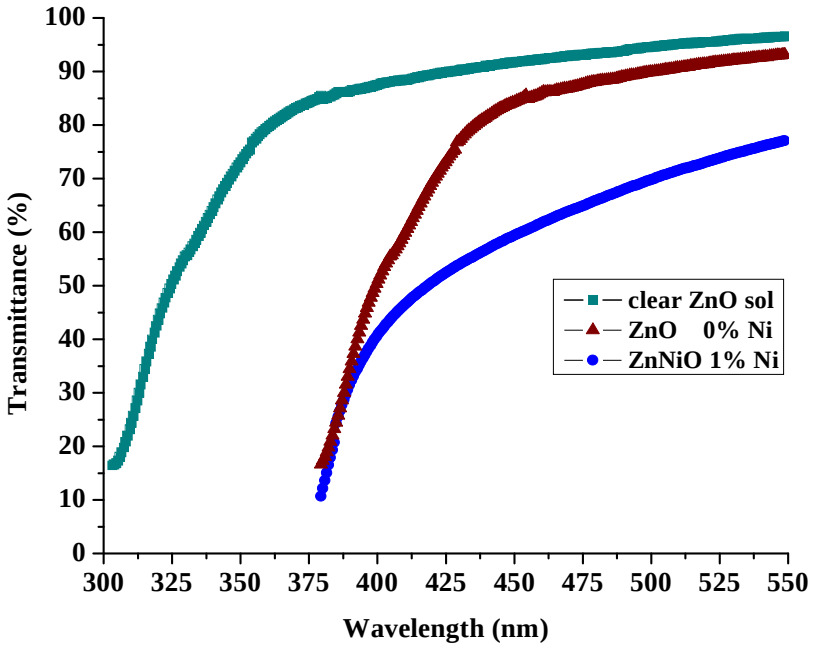

Fig. 6: Transmittance spectra of clear ZnO sol, undoped ZnO and Ni doped ZnO thin films as a function of wavelength (λ).

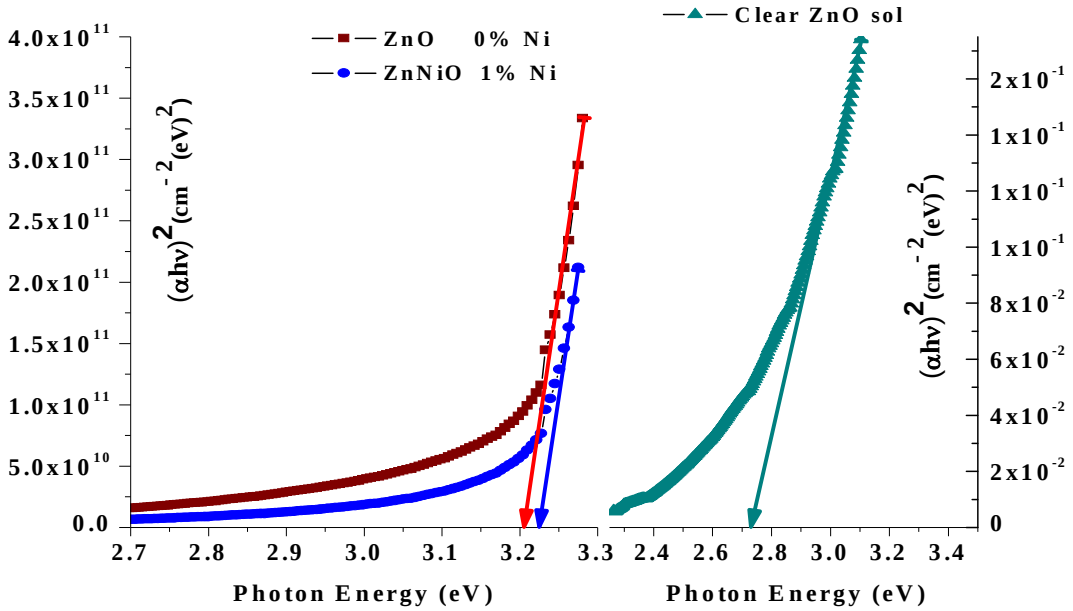

Fig. 7: Plot of $(\alpha h\nu)^2$ vs. Photon energy ($h\nu$) showing variation of band gap with Ni doping annealed at 600 ºC and inset shows the band gap of 2.73 eV of clear ZnO sol before spin coating.

The band gap was estimated by extrapolation of linear portion of $(\alpha h\gamma)^2$ versus $h\gamma$ curve (Fig. 7) by using the Tauc plot relation

$$(\alpha h\gamma)^2 = B(h\gamma - E_g) \tag{7}$$

for the direct band gap semiconductor between the absorption coefficient (α) and the optical energy band gap (E_g), where h is the Planck's constant and γ is the frequency of the incident photon and B is a constant. Band gaps are observed to vary from 3.21eV for ZnO to 3.23 eV for Ni-doped ZnO thin films annealed at 600ºC with increase of the nickel concentration as shown in the Fig. 7. This optical energy band gap widening and the absorption edge blue shift can be attributed to an increase in the carrier concentration and principle can be explained by the Moss-Burstein band filling effect, which is frequently observed in n-type semiconductors.

IV. CONCLUSIONS

The structural and optical characterisation of nanocrystalline ZnO and Ni doped ZnO thin films grown by sol-gel spin coating using X-ray diffraction, HRTEM and UV-VIS double beam spectrophotometer have been investigated. The substitution of Zn sites by Ni^{2+} ions in wurtzite ZnO was confirmed by XRD. The SAED pattern confirms the nano particles are polycrystalline nature. The low magnification TEM images show the nano crystalline are hexagonal and the HRTEM analysis shows the inter planer spacing of the lattice planes. Blue shift in the band gap with Ni doping has been observed which may be due to the Moss-Burstein band filling effect.

V. ACKNOWLEDGEMENT

The author is again thankful to UGC, India for financial support under minor research project of reference number F. PSW-135/13-14.

REFERENCES

[1] Yu-Lin Wang, H. S. Kim, D. P. Norton[1], S. J. Pearton, and F. Ren "Dielectric passivation effects on ZnO light emitting diodes" Appl. Phys. Lett., Vol. 92, 112101, 2008.
[2] David C. Look, "Progress in ZnO materials and devices" Journal of Electronic Materials, Vol. 35, issue 6, pp. 1299-1305, 2006.
[3] N. G. Dhere, "Present status and future prospects of CIGSS thin film solar cells," Solar Energy Materials and Solar Cells, Vol. 90, No. 15, pp. 2181-2190, 2006.
[4] N. F. Cooray, et al., "Large area ZnO films optimized for graded band-gap Cu(InGa)Se2-based thin-film mini- modules," Solar Energy Materials and Solar Cells, Vol. 49, No. 1-4, pp. 291-297, 1997.

[5] Y. Hagiwara, T. Nakada and A. Kunioka, "Improved J_{SC} in CIGS thin film solar cells using a transparent conducting ZnO:B window layer," Solar Energy Materials and Solar Cells, Vol. 67, No. 1-4, pp. 267- 271, 2001.
[6] N. Saito, H. Haneda, T. Sekiguchi, N. Ohashi, I.Sakaguchi and K. Koumoto, "Low-temperature fabrication of light emitting zinc oxide micropatterns using self-assembled monolayers," Advanced Materials,14, pp. 418-421, 2002.
[7] M. H. Huang, S. Mao, H. Feick, H. Yan, Y. Wu, H. Kind,E.Weber,R.RussoandP.Yang, "Room temperature ultraviolet nanowire nanolasers," Science, 292, pp. 1897-1899, 2001.
[8] T. Meron and G. Markovich, "Ferromagnetism in colloidal Mn2+-doped ZnO nanocrystals," Journal of Physical Chemistry B, Vol. 109, No. 43, pp. 20232-20236, 2005.
[9] S. T. Shishiyanu, T. S. Shishiyanu and O. I. Lupen, "Sensing characteristics of tin-doped ZnO thin films as NO_2 gas sensor," Sensors and Actuators B: Chemical, Vol. 107, No. 1, pp. 379-386, 2005.
[10] S. J. Kang, J. Y. Choi, D. H. Chang and Y. S. Yoon, "A study on the growth and piezoelectric characteristics of ZnO thin film using a RF magnetron sputtering method," Journal of Korean Physics Society, Vol. 47, No. 93, pp. S589-S594, 2005.
[11] P. Nunes, D. Costa, E. Furtunato and R. Martins, "Performances presented by zinc oxide thin films deposited by R. F. magnetron sputtering," Vacuum, Vol. 64, No. 3- 4, pp. 293-297, 2002.
[12] K. Tominaga, T. Takao, A. Fukushima, T. Moriga and I. Nakabayashi, "Amorphous ZnO-In2O3 transparent conductive films by simultaneous sputtering method of ZnO and In2O3 targets," Vacuum, Vol. 66, No. 3-4, pp. 505-509, 2002.
[13] N. Naghavi, C. Marcel, L. Dupont, A. Rougier, J. B. Leriche and C. Guery, "Structural and physical characterization of transparent conducting pulsed laser deposited In2O3-ZnO thin films," Journal of Materials Chem- istry, Vol. 10, No. 10, pp. 2315-2319, 2000.
[14] M. Krunks and E. Mellikov, "Zinc oxide thin films by the spray pyrolysis method," Thin Solid Film, Vol. 270, No. 1-2, pp. 33-36, 1995.
[15] Y. Natsume and H. Sakata, "Electrical and optical properties of zinc oxide films post-annealed in H_2 after fabrication by sol-gel process," Materials Chemistry and Physics, Vol. 78, No. 1, pp. 170-176, 2002.
[16] E. J. Luna-Arredondo, A. Maldonado, R. Asomoza, D. R. Acosta, M. A. Melendez-Lira and M. de la L. Olvera, "Indium-doped ZnO thin films deposited by the sol-gel technique," Thin Solid Films, Vol. 490, No. 2, pp. 132-136, 2005.
[17] N. R. S. Farley, C. R. Staddon, L. X. Zhao, K. W. Edmunds, B. L. Gallagher and D. H. Gregory, "Sol-gel formation of ordered nanostructured doped ZnO films," Journal of Materials Chemistry, Vol. 14, No. 7, pp. 1087-1092, 2004.
[18] M. Ohyama, H. Kozuka and T. Yoko, "Sol-gel preparation of ZnO films with extremely preferred orientation along (002) plane from zinc acetate solution" , Thin Solid Films, Vol. 306, No. 1, pp. 78-85, 1997.
[19] E. J. Gonzalez, J. A. S. Urueta and R. S. Parra, "Optical and electrical characteristics of aluminum-doped ZnO thin films prepared by sol-gel technique," Journal of Crystal Growth, Vol. 192, No. 3-4, pp. 430-438, 1998.
[20] Z. R. Khan, M. Zulfequar and M. S. Khan, "Optical and structural properties of thermally evaporated cadmium sulphide thin films on silicon (100) wafers," Materials Science and Engineering: B, Vol. 174, No. 1-3, pp. 145-149, 2010.

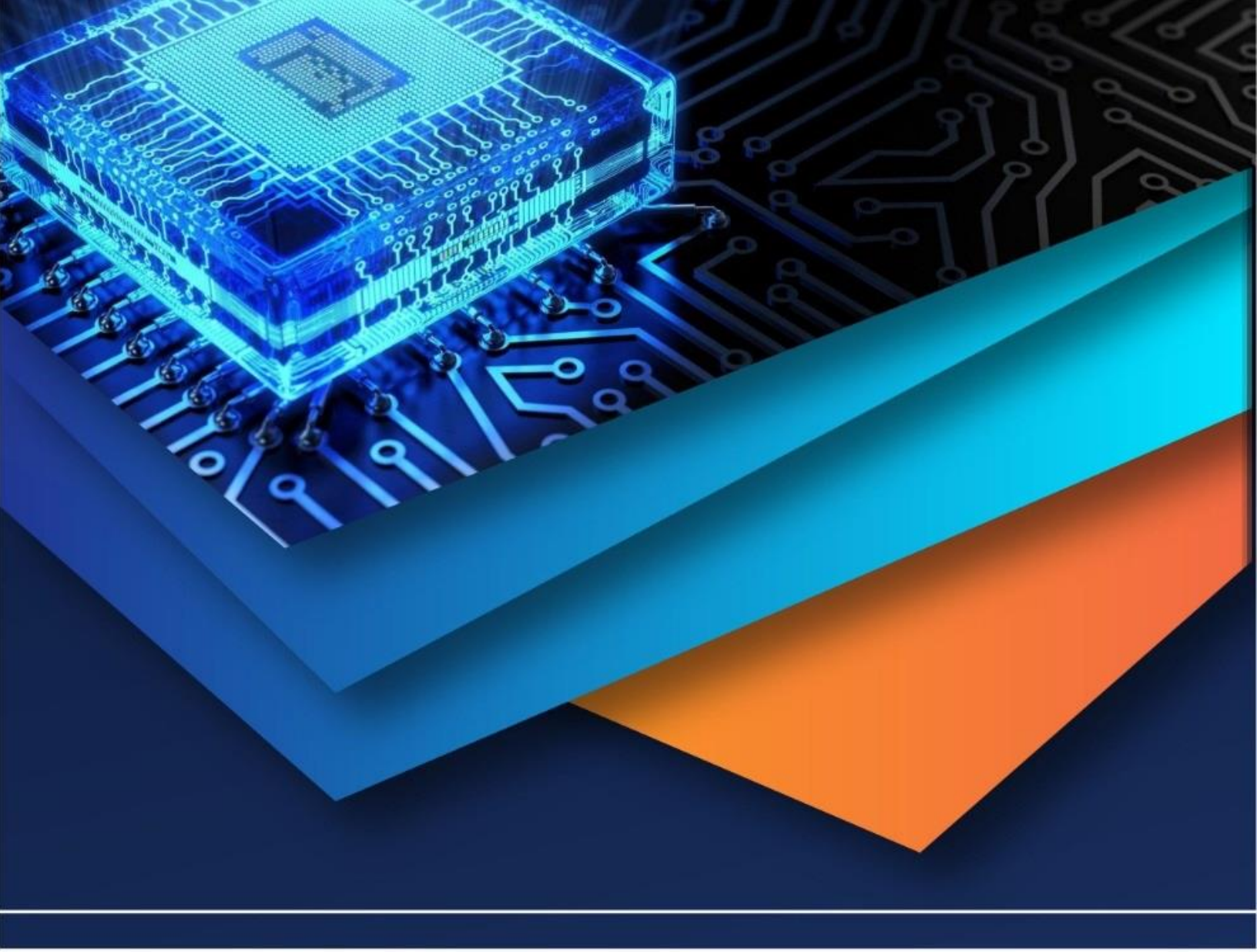

10.22214/IJRASET

45.98

IMPACT FACTOR: 7.129

IMPACT FACTOR: 7.429

INTERNATIONAL JOURNAL FOR RESEARCH

IN APPLIED SCIENCE & ENGINEERING TECHNOLOGY